Available online at www.sciencedirect.com

SciVerse ScienceDirect

Nuclear Medicine and Biology 39 (2012) 247–260

NUCLEAR MEDICINE — AND — BIOLOGY

www.elsevier.com/locate/nucmedbio

Radiohalogenated 4-anilinoquinazoline-based EGFR-TK inhibitors as potential cancer imaging agents

Carina Neto[a], Célia Fernandes[a], Maria Cristina Oliveira[a,*], Lurdes Gano[a], Filipa Mendes[a], Torsten Kniess[b], Isabel Santos[a]

[a]*Unidade de Ciências Químicas e Radiofarmacêuticas, Instituto Tecnológico e Nuclear, Estrada Nacional 10, 2686-953 Sacavém, Portugal*
[b]*Institute of Radiopharmacy, Helmholtz-Zentrum Dresden-Rossendorf e.V., POB 510119, D-01314 Dresden, Germany*

Received 7 March 2011; received in revised form 9 September 2011; accepted 12 September 2011

Abstract

Introduction: The overexpression of epidermal growth factor receptor (EGFR) in tumors underlines the recent interest in EGFR as attractive target for the development of new cancer imaging agents. EGFR-tyrosine kinase inhibitors (EGFR-TKIs) based on the anilinoquinazoline scaffold have been explored as potential probes for EGFR imaging. However, up to now, no optimal radiotracer is available. Herein, we report the synthesis and biological evaluation of three novel halogenated 6-substituted 4-anilinoquinazoline based EGFR-TKIs. Radiosynthesis (^{125}I and ^{18}F) of the corresponding analogues was also performed.

Methods: 6a, **6b** and **8** were obtained by reaction of 6-amino-4-anilinoquinazoline (**5**) with 3-/4-iodobenzoyl and 4-fluorobenzoyl chlorides. Inhibition of EGFR autophosphorylation and A431 cellular proliferation were assessed by Western blot and MTT assays. ^{125}I-anilinoquinazolines [^{125}I]**6a/b** were prepared via destannylation of the corresponding tributylstannyl precursors with [^{125}I]NaI. Cellular uptake studies were conducted in A431 cells. Optimization of the radiosynthesis of the ^{18}F-anilinoquinazoline [^{18}F]**8** was attempted by nucleophilic substitution of the trimethylammonium- and nitro-6-substituted 4-anilinoquinazoline precursors.

Results: 6a, **6b** and **8** were synthesized in high chemical yield. All of them are inhibitors of EGFR autophosphorylation ($0.1<IC_{50}<1$ μM) and A431 cell proliferation ($IC_{50}<3.5$ μM). [^{125}I]**6a/b**, obtained in high radiochemical purity and specific activity, were highly taken up by A431 cells. Biodistribution profile in mice indicated fast blood clearance and hepatobiliary excretion. Despite all attempts, **[^{18}F]8** was only formed in 4% yield, hampering further biological evaluation.

Conclusions: This study suggests that these quinazoline derivatives can act as EGFR-TKI, warranting further modifications in the chemical structure in order to be explored as potential molecular imaging agents for single photon emission computerized tomography and positron emission tomography.

© 2012 Elsevier Inc. All rights reserved.

Keywords: 4-Anilinoquinazolines; EGFR-TK inhibitors; Radiohalogenation; SPECT; PET; Iodine-125; Fluorine-18

1. Introduction

Conventional therapies like surgery, radiation therapy and chemotherapy have been up to now the standard approaches for treatment of several types of tumors and have led to improved survival of cancer patients. Nevertheless, treatment-related toxicity and its side effects, lack of specificity, as well as drug resistance development often hamper the therapeutic effectiveness and have been a major cause of morbidity and mortality. So, more effective and specific cancer therapies are needed to improve patient outcome. Recent scientific advances in the understanding of cancer biology have allowed the identification of several oncogenic pathways which are deregulated in malignant cells and represent potential new targets for tumor therapy. Among them, the protein tyrosine kinases (TKs) have emerged as ubiquitous but very challenging targets due to their important role in tumor signal transduction pathways and in the development and maintenance of different types of tumors. Especially, the epidermal growth factor receptor (EGFR) that belongs to the human epidermal receptor (HER) family is one of the most widely studied TKs due to its overexpression

* Corresponding author. Tel.: +351 219946184; fax: +351 219946185.
E-mail address: cmelo@itn.pt (M.C. Oliveira).

0969-8051/$ – see front matter © 2012 Elsevier Inc. All rights reserved.
doi:10.1016/j.nucmedbio.2011.09.001

and enhanced signaling connected to cancer [1,2]. As tyrosine phosphorylation is a primary pathway associated to signal transduction through the cell membrane to the nucleus, any TK malfunction can lead to malignant pathogenesis as a result of overexpression or mutational activation of TK receptors [3].

Two promising receptor TK-targeted therapeutic approaches include monoclonal antibodies to target membrane receptor domains and inhibit cancer cell growth, and small molecule inhibitors of tyrosine kinase activity (TKIs) that act as competitive inhibitors at the adenosine triphosphate (ATP) binding site in the intracellular catalytic domain and disrupt the signal transduction pathway [4,5]. Even so, only few TKIs have been approved for clinical studies. Moreover, the use of those TKIs has induced in some patients the appearance of drug-resistant tumors, which have been attributed to several mechanisms like amplification of oncogenic genes or amino acid mutations in the kinase domain. Consequently, mutant drug targets present altered binding properties, resulting in insufficient and unpredictable clinical response. These findings have motivated intense research efforts on the design of novel therapeutic compounds for targeting TK receptors with enhanced biological behavior.

Gefitinib and erlotinib are approved drugs from the class of the 4-anilinoquinazolines, effective in the treatment of non-small-cell lung cancer by reversibly inhibiting EGFR [6]. Their clinical outcome has led to the design of other TKIs based on the anilinoquinazoline scaffold that compete with ATP [7,8]. In order to overcome drug resistance to reversible inhibitors, the search has also been directed towards irreversible binding inhibitors, such as canertinib, which irreversibly inhibits EGFR and other HERs [9]. Irreversible inhibitors have also the advantage of prolonged clinical effects and need for less frequent dosing. However, it may compromise specificity and tolerability [10]. Alternative TKIs such as lapatinib have been developed. This is the first dual inhibitor of EGFR and HER2, approved in 2007, for co-adjuvant targeted therapy of patients with advanced breast cancer or metastatic cancer and whose tumors express HER2 (Fig. 1) [11,12].

Clinical studies with these drugs made evident that the responsiveness to therapy is related with EGFR mutations. Several mutated forms of the EGFR resulting from either deletions on the extracellular domain (namely, EGFRvI, vII and vIII) or mutations in the ATP-binding and catalytic regions of the TK domain have been reported. Different mutations might result in different tumor dependency, and to achieve effective targeted therapy, feasible information about the expression/activity of EGFR at the kinase level is required to determine which patients are most likely to benefit from each therapeutic approach [13,14]. Thus, noninvasive molecular imaging of EGFR in tumors could help in the assessment of this information.

In particular, the labeling of TKI with radionuclides for single photon emission computerized tomography (SPECT) or positron emission tomography (PET) may lead to suitable probes for early detection and staging of cancer [15–22]. Such predictive radiotracers would provide unique information about EGFR status in tumors of individual patients, helping to select cancer patients for treatment with TKI inhibitors and monitor their therapeutic response.

Although some of the proposed TKI radiotracers are based on approved drugs, they often, for a number of reasons, did not yield adequate SPECT/PET imaging. Therefore, the chemical structures of some TKI have been modified to act as suitable radioactive probes. Several inhibitors, particularly from the 4-anilinoquinazoline class, were labeled with SPECT and PET radionuclides [23–35]. However, until now, none of them has shown a suitable biological profile for molecular imaging of EGFR in cancer. Further studies and more efforts are required in order to

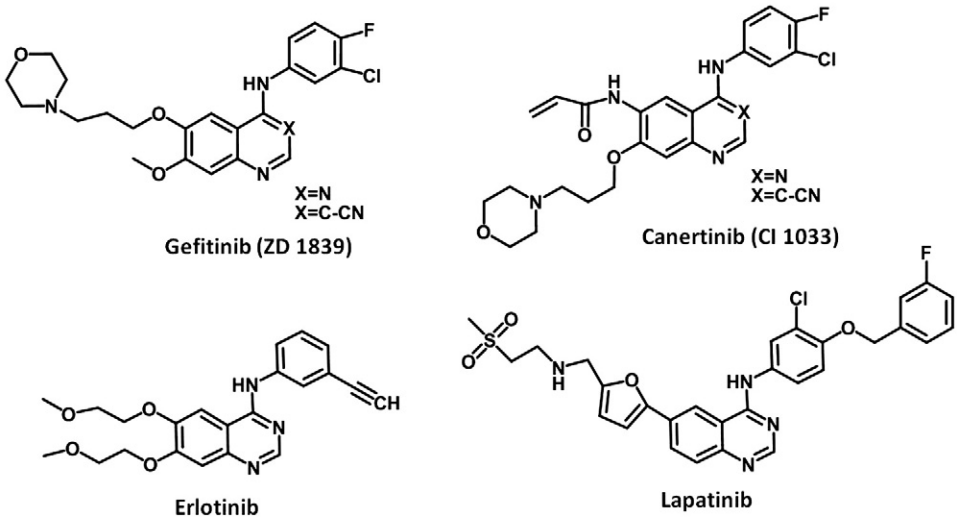

Fig. 1. Representative chemical structures of some EGFR-TKIs drugs.

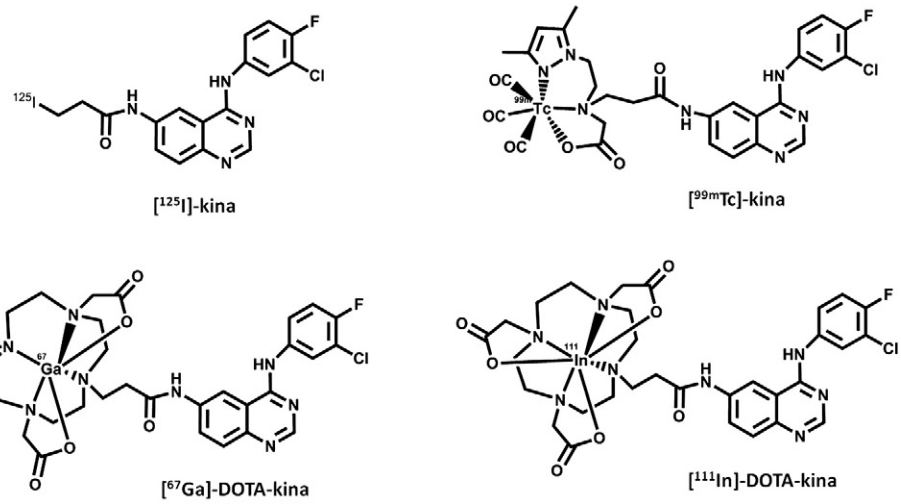

Fig. 2. Chemical structures of radiolabeled 4-anilinoquinazoline derivatives for SPECT imaging: [^{125}I]-kina [23], [^{99m}Tc]-kina [24], [^{67}Ga]-DOTA-kina [26] and [^{111}In]- DOTA-kina [27].

widen our knowledge on structure/activity relationships, an important issue for possible clinical translation.

We have previously studied and evaluated in vitro and in vivo ^{125}I-, ^{99m}Tc-, ^{67}Ga- and ^{111}In-labeled quinazoline derivatives potentially applicable for early SPECT detection and staging of EGFR-positive tumors (Fig. 2) [23,24,26,27]. In the case of ^{125}I, we have evaluated a 4-anilinoquinazoline derivative of gefitinib bearing an iodopropionamide substituent at the C6 quinazoline scaffold. In vitro studies indicated that the cold compound inhibited A431 cell growth and EGFR autophosphorylation, but in vivo stability assays suggested a fast deiodination [23].This is probably due to the low chemical stability of the aliphatic carbon-iodine bond, so we have hypothesized that the use of an iodobenzamide chain could increase the in vivo stability.

In our search for the development of SPECT/PET radioligands for early detection and staging of EGFR-positive tumors, novel radioiodinated and radiofluorinated probes based on quinazoline TKI activity have been explored. Herein, we report the synthesis and biological evaluation of three novel halogenated 6-substituted 4-anilinoquinazoline-based EGFR-TK inhibitors. To gain a first insight into the potential relevance of the iodinated quinazolines as probes for EGFR-TKI targeting, cellular uptake studies in A431 cells and biodistribution assays with the corresponding radioiodinated analogues have also been performed. This paper also describes the studies undertaken to prepare the radiofluorinated analogue of the fluorinated quinazoline.

2. Materials and methods

2.1. General

All commercial reagents and solvents were of analytical grade and were used without further purification. High-performance liquid chromatography (HPLC)-grade solvents were used for HPLC purification and analysis. No-carrier-added sodium[^{125}I]-iodide (17.4 Ci/mg) in 0.1 M aqueous NaOH was obtained from Perkin Elmer-Life, USA. Analytical thin-layer chromatography was run using Merck 60 F 254 silica gel plates, and spots were visualized under UV light (254 nm). Purification of intermediate or final products was performed by column chromatography using silica gel (70-230 mesh) from Merck.

Proton and carbon nuclear magnetic resonance spectra (^{1}H and ^{13}C) were performed on a Varian Unity 300-MHz spectrometer using DMSO-d_6 as solvent. Electron impact mass spectra were acquired by Electrospray ionisation/Quadrupole ion trap mass spectrometry (ESI/-QITMS) from a Bruker HCT Mass Spectrometer. C, H, N analyses were performed using a CE Instruments EA 110 automatic analyzer.

High-performance liquid chromatography analyses were performed on a Perkin-Elmer system equipped with a biocompatible quaternary pump (series 200), a UV/vis detector (SPD-10 AV, Shimadzu, UV detection at 254 nm) and a radioactivity detector (LB 509, Berthold). Purification of radioiodinated compounds and analysis of the final products were carried out by analytical reverse-phase HPLC on an EC-Nucleosil C18 column (250/4 mm, 10 μm, Macherey Nagel) with a flow rate of 0.5 ml/min by isocratic elution with acetonitrile with 0.1% trifluoroacetic acid (TFA) and 0.1% aqueous TFA.

No-carrier-added aqueous [^{18}F]fluoride ion was produced in an IBA CYCLONE 18/9 cyclotron by irradiation of [^{18}O]H_2O via the ^{18}O(p,n)^{18}F nuclear reaction. The drying procedure of [^{18}F]fluoride, the formation of the reactive [^{18}F]fluoride-K_2CO_3/K_{222} complex and the fluorination experiments were performed in an automated nucleophilic fluorination module (Nuclear Interface, Münster, Germany). The *N*-succinimidyl 4-[**^{18}**F]fluorobenzoate ([^{18}F]SFB) was

produced in an automated synthesizer module according a published procedure [36]. Analytical HPLC analyses were carried out with a Discovery C18 column (150/4 mm, 5 μm, Supelco) using an isocratic elution method with acetonitrile and 0.1% aqueous TFA by gradient pump L2500 (MERCK, HITACHI). The products were monitored by UV detector L4500 (MERCK, HITACHI) at 254 nm and by gamma-detection with scintillation detector GABI (Raytest,Agilent Technologies).

2.2. Chemistry

2.2.1. N-{4-[(3-chloro-4-fluorophenyl)amino]quinazoline-6-yl}-3-iodobenzamide (6a)

To a solution of 6-amino-4-[(3-chloro-4-fluorophenyl) amino]quinazoline (**5**) (342 mg, 1.2 mmol) were slowly added 3-iodobenzoyl chloride (693 mg, 2.6 mmol) and triethylamine (0.2 ml) in dry acetone (15 ml). The reaction mixture was left under stirring at room temperature for 40 min and was followed by thin-layer chromatography in acetonitrile/dichloromethane (1:3) until a yellow precipitate was formed. The precipitate was separated by filtration and dried under reduced pressure to give **6a** (589 mg, 1.14 mmol) as a yellow solid in 96% yield. ^{1}H NMR (300 MHz, DMSO-d_6) 7.39 (t, 1H), 7.55 (t, 1H), 7.70 (m, 1H), 8.02 (m, 2H), 8.20 (dd, 1H, *J*=2.1 Hz, *J*=8.8 Hz), 8.40 (s, 1H), 8.89 (s, 1H), 9.14 (d, 1H, *J*=1.8 Hz), 10.94 (s, 1H). ^{13}C NMR (75 MHz, DMSO-d_6) 95.00, 113.96, 114.39, 117.00 (d, $J^{F\text{-}C=}$22.0 Hz), 119.14, 119.38, 120.89, 125.51, 125.60, 126.88, 127.43, 130.81, 134.20, 135.93, 136.10, 138.77, 140.72, 149.98, 155.29 (d, $J^{F\text{-}C}$=245.5 Hz), 159.72, 164.32. **IR** (KBr) (cm^{-1}): 1674.6 (vs); 1566.6 (s); 1208.6 (s). Analytically calculated for $C_{21}H_{13}ClFIN_4O$+HCl: C, 45.43; H, 2.54; N, 10.09. Found: C, 45.32; H, 2.76; N, 10.24. ESI/MS: *m*/*z* (% int) 518.8 (100) $[M+H]^+$.

2.2.2. N-{4-[(3-chloro-4-fluorophenyl)amino]quinazoline-6-yl}-4-iodobenzamide (6b)

Identically as described for the synthesis of **6a**, *N*-{4-[(3-chloro-4-fluorophenyl)amino]quinazoline-6-yl}-4-iodobenzamide (**6b**) was prepared by adding slowly 4-iodobenzoyl chloride (405 mg, 1.5 mmol) to a solution of **5** (200 mg, 0.7 mmol) and triethylamine (0.2 ml) in dry acetone (15 ml). The reaction mixture was left under stirring at room temperature for 40 min and was followed by thin-layer chromatography in acetonitrile/dichloromethane (1:3) until a yellow precipitate was formed. The precipitate was separated by filtration and dried under reduced pressure to give **6b** (340 mg, 0.66 mmol) as a yellow solid in 95% yield. ^{1}H RMN (300 MHz, DMSO-d_6) 7.53 (t, 1H), 7.71 (m, 1H), 7,86 (d, 2H, *J*=8.7 Hz), 7.98 (m, 4H), 8.23 (dd, 1H, *J*=1.8 Hz, *J*=9.3 Hz), 8.87 (s, 1H), 9.14 (d, 1H, *J*=2.1 Hz), 10.98 (s, 1H). ^{13}C NMR (75 MHz, DMSO-d_6) 100.99, 114.66, 114.86, 117.68 (d, $J^{F\text{-}C}$=21.4 Hz), 119.82, 120.06, 121.79, 126.12, 126.22, 127.51, 130.44, 131.36, 133.96, 134.90, 136.72, 138.21, 139.47, 150.77, 155.93 (d, $J^{F\text{-}C}$=245.5 Hz), 160.34, 165.89. Analytically calculated for $C_{21}H_{13}ClFIN_4O$+2HCl: C, 42.63; H, 2.56; N, 9.47. Found: C, 42.80; H, 2.31; N, 9.67. ESI/MS: *m*/*z* (% int) 518.8 (100) $[M+H]^+$.

2.2.3. N-{4-[(3-chloro-4-fluorophenyl)amino]quinazoline-6-yl}-3-(trimethylstannyl) benzamide (7a)

To a solution of **6a** (40 mg, 0.08 mmol) in dry toluene (8 ml) were added hexamethylditin (109 μl, 0.52 mmol) and a catalytic amount of tetrakis(triphenylphosphane)palladium(0). The reaction mixture was stirred under a nitrogen atmosphere at reflux temperature for 16 h. The mixture was cooled to room temperature and filtered through celite, and the solvent was removed in vacuum. The crude was purified by column chromatography using chloroform/methanol (9:1) to give **7a** (10.7 mg, 0.020 mmol) as a yellow solid in about 25% yield. ESI/MS: *m*/*z* (% int.) 579.0 (100) $[M+Na]^+$. HPLC, R_T=13.54 min [CH_3CN with 0.1% TFA/0.1% aqueous TFA (65/35)].

2.2.4. N-{4-[(3-chloro-4-fluorophenyl)amino]quinazoline-6-yl}-4-(trimethylstannyl) benzamide (7b)

Identically as described for the synthesis of **7a**, *N*-{4-[(3-chloro-4-fluorophenyl)amino]quinazoline-6-yl}-4-(trimethylstannyl)benzamide (**7b**) was prepared by reacting **6b** (75 mg, 0.14 mmol) in dry toluene (8 ml) with hexamethylditin (187 μl, 0.9 mmol) and a catalytic amount of tetrakis(triphenylphosphane)palladium(0). The reaction mixture was stirred under a nitrogen atmosphere at reflux temperature for 16 h. The mixture was cooled to room temperature and filtered through celite, and the solvent was removed in vacuum. The crude was purified by column chromatography using chloroform/methanol (95/5) to afford **7b** (16.1 mg, 0.03 mmol) as a yellow solid in about 20% yield. ESI/MS: *m*/*z* (% int.) 579.0 (100) $[M+Na]^+$. HPLC, R_T=19.60 min [CH_3CN with 0.1% TFA/0.1% aqueous TFA (60/40)].

2.2.5. N-{4-[(3-chloro-4-fluorophenyl)amino]quinazoline-6-yl}-4-fluorobenzamide (8)

To a solution of **5** (200 mg, 0.69 mmol) and triethylamine (0.28 ml) in dry acetone (15 ml) was slowly added 4-fluorobenzoyl chloride (237 mg, 1.5 mmol). The reaction mixture was left under stirring at room temperature for 2 h until a yellow precipitate was formed. After completion, the precipitate was separated by filtration and dried under reduced pressure to give **8** (263 mg, 0.64 mmol) as a yellow solid in 93% yield. The compound was characterized and used without further purification. ^{1}H RMN (300 MHz, DMSO-d_6) 7.40-7.46 (m, 3H), 7.56 (t, 1H), 7.68-7.72 (m, 1H), 7.97-8.02 (m, 2H), 8.13-8.23 (m, 3H), 8.91 (s, 1H), 9.18 (s, 1H), 10.94 (s, 1H). ^{13}C NMR (75 MHz, DMSO-d_6) 114.76, 116.33 (d, $J^{F\text{-}C}$=21.9 Hz), 117.65 (d, $J^{F\text{-}C}$=21.9 Hz), 119.79, 120.04, 125.90, 126.01, 127.29, 128.18, 129.08, 131.12, 131.27, 131.40, 135.07, 139.44, 151.02, 155.81 (d, $J^{F\text{-}C}$=245 Hz), 161.83 (d, $J^{F\text{-}C}$=245 Hz), 165.42. ^{19}F RMN (282 MHz, DMSO-d_6) -119.23, -108.18. Analytically calculated for $C_{21}H_{13}ClF_2N_4O$+HCl: C, 56.39; H, 3.16; N,

12.56. Found: C, 56.33; H, 2.96; N, 12.56. ESI/MS: *m/z* (% int.) 408.9 (100) $[M-H]^-$.

2.2.6. *N-{4-[(3-chloro-4-fluorophenyl)amino]quinazoline-6-yl}-4-dimethylamino-benzamide(**9**)*

To a solution of **5** (200 mg, 0.69 mmol) and triethylamine (0.29 ml) in dry acetone (20 ml) was slowly added 4-(dimethylamino) benzoyl chloride (250 mg, 1.4 mmol). The reaction mixture was left overnight under stirring at room temperature until a yellow precipitate was formed. After completion, the precipitate was separated by filtration and dried under reduced pressure to give **9** (177 mg, 0.40 mmol) as a yellow solid in 59% yield. The compound was used without further purification in the next reaction step. ^{1}H RMN (300 MHz, DMSO-d_6) 3.01 (s, 6H), 6.79 (d, *J*=8.7 Hz), 7.44 (t, 1H), 7.77-7.84 (m, 2H), 7.95 (d, 2H, *J*=8.7 Hz), 8.02 (m, 1H), 8.17 (d, 1H), 8.56 (s, 1H), 8.87 (s, 1H), 9.94 (s, 1H), 10.24 (s, 1H). ^{13}C NMR (75 MHz, DMSO-d_6) 39.9, 111.54, 117.21 (*J*=21.4 Hz), 119.28, 119.53, 121.00, 123.11, 123.21, 124.28, 128.80, 129.11, 129.92, 137.48, 138.16, 147.16, 153.24, 155.79 (d, *J*=245 Hz), 165.94. Analytically calculated for $C_{23}H_{19}ClFN_5O$+3HCl: C, 50.66; H, 4.07; N, 12.85. Found: C, 50.47; H, 4.01; N, 12.59. ESI/MS: *m/z* (% int.) 470.3 (100) $[M+Cl]^-$.

2.2.7. *N-{4-[(3-chloro-4-fluorophenyl)amino]quinazoline-6-yl}-4-trimethylammonium-benzamide trifluoromethanesulfonate (**10**)*

To a solution of **9** (100 mg, 0.23 mmol) in dry tetrahydrofuran THF (20 ml) was added methyl trifluoromethanesulfonate (0.052 ml, 0.47 mmol). The reaction mixture was left overnight under stirring at room temperature. The solvent was evaporated, and the resulting crude was purified by column chromatography using THF/chloroform (8:1) to give **10** (67 mg, 0.11 mmol) as a yellow solid in 73% yield. ^{1}H RMN (300 MHz, DMSO-d_6) 3.60 (s, 9H), 6.76 (d, 2H, *J*=7.8 Hz), 6.97 (m, 2H), 7.21-7.29 (m, 2H), 7.45 (d, 1H), 7.92 (d, 2H, *J*=7.9 Hz), 7.98 (s, 1H), 8.22 (d, 1H), 8.61 (s, 1H), 10.16 (s, 1H). ^{13}C NMR (75 MHz, DMSO-d_6) 104.20, 111.56, 115.92, 117.64 (d, J^{F-C}=21.9 Hz), 118.77, 120.27, 122.37, 125.90, 127.84, 128.28, 130.63, 134.98, 145.88, 147.85, 149.67, 155.80 (d, J^{F-C}= 246 Hz), 159.12. ESI/MS: *m/z* (% int.) 450.0 (100) $[M]^+$.

2.2.8. *N-{4-[(3-chloro-4-fluorophenyl)amino]quinazoline-6-yl}-4-nitrobenzamide (**11**)*

To a solution of **5** (125 mg, 0.43 mmol) and triethylamine (180 μl) in dry THF (20 ml) was slowly added 4-nitro benzoyl chloride (156 mg, 0.84 mmol). The reaction mixture was left overnight under stirring at room temperature, and after completion, the precipitate was removed by filtration. The filtrate was evaporated to dryness, and the residue was purified by column chromatography using chloroform/-methanol (9/1), giving **11** (66 mg, 0.15 mmol) as a yellow solid in 35% yield. ^{1}H RMN (300 MHz, DMSO-d_6) 3.44 (t, 1H), 7.85 (m, 2H), 8.01 (m, 1H), 8.15 (m, 1H), 8.26 (d, 2H, *J*=8.7 Hz), 8.42 (d, 2H, *J*=8.7 Hz), 8.59 (s, 1H), 8.90 (s, 1H), 10.00 (s, 1H), 10.95 (s, 1H). ^{13}C NMR (75 MHz, DMSO-d_6) 114.27, 115.74, 117.28 (d, *J*=21.4 Hz), 123.54, 123.63, 124.43, 124.71, 129.00, 129.90, 136.97, 140.70, 147.47, 150.00, 152.60, 156.18 (d, *J*=258.3 Hz), 165.09. Analytically calculated for $C_{21}H_{13}ClFN_5O_3$+HCl: C, 53.18; H, 2.98; N, 14.77. Found: C, 53.23; H, 3.07; N, 14.90. ESI/MS: *m/z* (% int.) 438.6 (81.5) $[M+H]^+$.

2.3. Radiochemistry

2.3.1. Radioiodination

To a solution containing stannyl precursor, **7a** or **7b** (≈100 μg, 0.18 μmol) in 100 μl of methanol was added 100 μl of an oxidant solution consisting of 30% hydrogen peroxide/acetic acid (1/3) and [^{125}I]NaI (≈5 μl, ≈35 MBq). The mixture was vortexed for 30 s and allowed to react for 10 min at room temperature. The reaction was diluted with 100 μl of water, and then 0.1 N HCl (100 μl) was added [37]. The suspension was loaded onto a C18 Sep-Pak cartridge (prewashed with 10 ml of methanol, followed by 3×8 ml of water). The cartridge was washed with 10 ml of water, and the radioiodinated product was eluted with 2 ml of methanol. Radiochemically and chemically pure radioiodinated products *N*-{4-[(3-chloro-4-fluorophenyl)amino]quinazoline-6-yl}-3-[^{125}I]iodobenzamide ([^{125}I]**6a**) and *N*-{4-[(3-chloro-4-fluorophenyl)amino]quinazoline-6-yl}-4-[^{125}I]iodobenzamide ([^{125}I]**6b**) were obtained after reverse phase high performance liquid chromatography (RP-HPLC) purification on a Nucleosil C18 column (250/4 mm, 10 μm) with simultaneous UV (254 nm) and radioactivity detection by isocratic elution with acetonitrile containing 0.1% TFA and 0.1% aqueous TFA (65/35 and 60/40) for [^{125}I]**6a** and [^{125}I]**6b**, respectively, at a flow rate of 0.5 ml/min (R_T [^{125}I]**6a**=9.30 min; R_T [^{125}I] **6b**=10.78 min).

2.3.2. Radiofluorination

2.3.2.1. Labeling experiments with [^{18}F]fluoride-K_2CO_3/K_{222} complex. No-carrier-added aqueous [^{18}F]fluoride ion was produced in an IBA CYCLONE 18/9 cyclotron by irradiation of [^{18}O]H_2O via the ^{18}O(p,n)^{18}F nuclear reaction. The aqueous [^{18}F]fluoride (300–500 MBq) was fixed on an anion exchange cartridge (QMA plus, Waters) and resolubilized by a solution of Kryptofix 222 and K_2CO_3. Removal of water was accomplished by azeotropic distillation with acetonitrile in a stream of nitrogen. Finally, the dried [^{18}F] KF/K_{222} complex was dissolved in 1 ml of anhydrous solvent (acetonitrile, dimethylformamide (DMF), dimethylsulfoxide (DMSO)) and heated in the presence of 5–15 mg of the appropriate precursors **10** and **11** for 20 min at the indicated temperatures. After cooling, the mixture was diluted with 2 ml of water, and the products were analyzed by analytical HPLC on a Discovery RP-C18 column (150/4 mm, 5 μm, Supelco) using an isocratic elution method with acetonitrile and 0.1% aqueous TFA (45/55) with simultaneous UV (254 nm) and gamma detection at a flow rate of 0.5 ml/min.

2.3.2.2. Labeling experiments with N-succinimidyl 4-[^{18}F] fluorobenzoate [^{18}F]SFB. A total of 250 MBq of [^{18}F] SFB in 150 μl of phosphate buffer pH=7.5 was incubated with 2 mg of 6-amino-4-[(3-chloro-4-fluorophenyl)amino] quinazoline (**5**) dissolved in 150 μl of DMSO at room temperature for 2 h. The course of reaction was monitored by analytical HPLC using the above described chromatographic conditions.

2.3.3. Estimation of lipophilicity

The lipophilicity, which is referred as to log $P_{o/w}$ (where P is the octanol-water partition coefficient) of the halogenated quinazolines, was determined from the log k'$_w$ values (k'$_w$=chromatographic capacity factor at 100% aqueous solution). These log k'$_w$ values were determined by reversed-phase HPLC on an EC-Nucleosil C-18 column (250/4 mm, 10 μm, Macherey Nagel) according to a method described by Minick et al. [38]. Measurement of the chromatographic capacity factors (k') for each compound was done at various concentrations in the range 85%–60% methanol (containing 0.25% octanol) and an aqueous phase consisting of 0.15% n-decylamine in 0.02 M MOPS (3-(*N*-morpholino)propanesulfonic acid) pH 7.4 (prepared in 1-octanol-saturated water). The compounds were dissolved at 1 mg/ml in methanol, and ≈5 μg was injected onto the column and eluted with a flow rate of 1 ml/min. The k' values are defined as $(R_T-t_0)/t_0$, where R_T and t_0 are the retention times of the compounds and nonretained species (solvent), respectively. The log k'$_w$ values were obtained from linear extrapolation of log k' vs. φ methanol (φ=volume fractions methanol) data acquired in the region $0.60 \leq \varphi$ methanol$\leq$0.85. The log $P_{o/w}$ values of the compounds were determined from a standard curve (log $P_{o/w}$ vs. log k'$_w$) constructed with data of standard compounds.

2.3.4. Human serum protein binding estimation and in vitro stability studies

The in vitro stability of the radioiodinated compounds was assessed in physiological saline and human serum by RP-HPLC using the chromatographic conditions above for the analysis of each compound. The experimental procedures used in these assays are described below.

2.3.4.1. Physiological saline. The radioiodinated quinazolines [^{125}I]**6a** and [^{125}I]**6b** (200 μL, ≈370 kBq) were incubated in physiological saline containing 1% Tween-20 at 6°C and at 37°C. Aliquots were taken before incubation started (for zero time point analysis) as well as at various time intervals during incubation (0, 1, 2, 4 and 24 h).

2.3.4.2. Human serum. The radioiodinated quinazolines [^{125}I]**6a** and [^{125}I]**6b** (100 μl, ≈370 kBq) in physiological saline (containing 1% Tween 20) were incubated in human serum (1 ml) at 37°C. At appropriate periods of time (0, 1, 2, 4 and 24 h), 100-μl aliquots (in duplicate) were sampled and treated with ethanol (200 μl) to precipitate the proteins. Samples were then cooled at 4°C and centrifuged at 3000 rpm for 15 min at 4°C. The supernatants were separated from the precipitate and analyzed by RP-HPLC using the experimental conditions described above. To estimate human serum protein binding, the precipitate was washed with ethanol (2×1 ml) and counted in a gamma counter (Berthold LB2111, Germany). The radioactivity in the precipitate was compared to the total activity used in the assay, and the percentage of radiolabeled quinazolines bound to proteins was calculated.

2.4. Biological evaluation

2.4.1. Cell line

Cellular studies were carried out in the EGFR-expressing cell line, A431, from a human epidermoid vulval carcinoma. Cells were grown in Dulbecco's Modified Eagle Medium (DMEM) medium containing Glutamax I (Invitrogen) supplemented with 10% fetal bovine serum and 1% penicillin/streptomycin under a humidified 5% CO_2 atmosphere at 37°C.

2.4.2. Inhibition of EGFR autophosphorylation

A431 cells (1×10^6) were seeded in a six-well plate and grown to 70% confluence. Cells were then incubated for 18 h in fresh medium without fetal bovine serum. The following day, cells were incubated with the quinazoline derivatives at concentrations ranging from 0.1 to 5 μM for 2 h and then stimulated with EGF (20 ng/ml) for 5 min. Controls consisted of wells without quinazoline derivatives and with or without EGF. The medium was removed, and cells were washed with cold PBS and lysed in Cell Lytic-Mammalian Tissue Extraction reagent (Sigma) supplemented with Complete protease inhibitor cocktail and Phosphatase inhibitor cocktail tablets (Roche Applied Science). After 15 min on ice, lysates were centrifuged at 14 000*g* for 10 min at 4°C to pellet the cellular debris, and the supernatants were removed for further use.

The total protein content was determined by using the DC Protein Assay Kit (Biorad), and aliquots of protein (30 μg) from each sample were analyzed using standard Western blot procedures. Briefly, protein extracts were subjected to electrophoresis on a 7% sodium dodecyl sulfate–polyacrylamide gel and transferred electrophoretically onto nitrocellulose membranes. The blots were blocked with PBS-T (PBS with 0,1% Tween 20) containing 5% nonfat dry milk for 1 h. Then, the blotting membranes were incubated with primary antibodies against phosphotyrosine (1:4000, Sigma) and actin (1:8000, Sigma) separately overnight. Membranes were washed with PBS-T and incubated for 1 h with secondary antibody (goat anti-mouse IgG-HRP, Biorad) diluted 1:3000. Finally, membranes were developed using the SuperSignal WetsPico Substrate kit (Pierce, Rockford, IL) according to the manufacturer's instructions. Band quantification was performed by densitometric analysis using AlphaView Software (Alpha Innotech), and the

percentage of EGFR autophosphorylation inhibition was calculated in comparison with the positive control (cells with EGF and without quinazoline derivatives).

2.4.3. Cell proliferation assay by MTT

A431 cells were seeded in a 96-well plate at a density of 7500 cells per 200 μl per well and incubated for 24 h for attachment to the wells. The day after seeding, exponentially growing cells were incubated with various concentrations of the quinazoline derivatives (**6a**, **6b** and **8**) (ranging from 1 nM to 100 μM in four replicates) for 72 h. Controls consisted of cells incubated in medium without any compound. The medium was removed, and the cells were incubated for 3 h in the presence of 0.5 mg/ml MTT (3-[4,5-dimethylthiazol-2-yl]-2,5-diphenyltetrazolium bromide, Sigma) in PBS (Invitrogen) at 37°C. The MTT solution was removed, and 200 μl per well of DMSO was added. After thorough mixing, absorbance of the wells was read in an enzyme-linked immunosorbent assay reader at test and reference wavelengths of 570 nm. The mean of the optical density of different replicates of the same sample and the percentage of each value were calculated (mean of the OD of various replicates/OD of the control). The percentage of the optical density against compound concentration was plotted on a semilog chart, and the IC_{50} from the dose–response curve was determined. Three cell proliferation assays were performed for each of the three compounds.

2.4.4. Cellular uptake studies

Cellular uptake studies of the radioiodinated quinazolines were accomplished with A431 cells plated at a density of 2×10^5 cells per 0.5 ml per well of a 24-well plate in culture medium. The day after seeding, the medium was removed and replaced by fresh medium containing approximately 5×10^5 cpm/0.5 ml of the radioiodinated quinazolines [^{125}I] **6a** and [^{125}I]**6b**. After 0.25, 0.5, 1, 2. 3 and 5 h of incubation at 37°C in humidified 5% CO_2 atmosphere, the cells were washed twice with cold PBS and lysed with 0.1 M NaOH, and the cellular extracts were counted for radioactivity in gamma counter (Berthold LB2111, Germany). Each experiment was performed in quadruplicate. Results of cell-associated radioactivity were expressed as the percentage of total cell radioactivity added, normalized per million of cells. Data, as mean values±S.D., are graphically presented as a function of incubation time.

2.4.5. Biodistribution and in vivo stability studies

In vivo studies were carried out in groups of four female CD-1 mice (randomly bred, obtained from IFFA, CREDO, Spain) weighing approximately 20–25 g. Animals were injected into the tail vein with 175–200 kBq of the radioiodinated compound in saline (100 μl) containing 1% Tween 20. Injected dose (ID) was assumed to be the difference between the measured radioactivity in the syringe before and after injection. Animals were maintained on normal diet ad libitum and were sacrificed by cervical dislocation at 1 and 4 h postinjection with the radiotracer. Tissue samples of the main organs were removed and weighed, and the activity was measured in a gamma counter (Berthold LB2111, Germany). Results were expressed as percentage of injected dose per total organ (%ID/organ) and/or per gram of organ (% ID/g) and were presented as mean values±S.D. For blood, bone and muscle, this value was calculated assuming that these organs constitute 6%, 10% and 40% of the total weight, respectively. Whole animal body radioactivity excretion was not quantified. The in vivo stability was evaluated by RP-HPLC analysis of urine samples collected at sacrifice in the experimental conditions described above for the radiochemical purity determination. Animal experiments were conducted in conformity with the national law and with the EU Guidelines for Animal Care and Ethics in Animal Experimentation.

3. Results and discussion

3.1. Chemistry

For in vitro biological evaluation studies and characterization of radiolabeled 4-anilino-quinazolines, the non-radioactive *N*-{4-[(3-chloro-4-fluorophenyl)amino] quinazoline-6-yl}-3-iodobenzamide **(6a)** and *N*-{4-[(3-chloro-4-fluorophenyl)amino]quinazoline-6-yl}-4-iodobenzamide **(6b)** were synthesized. The 4-fluorobenzyl substituted analogue *N*-{4-[(3-chloro-4-fluorophenyl)amino]-quinazoline-6-yl}-4-fluorobenzamide **(8)** was synthesized as well. The stannyl precursors **(7a/7b)** were also synthesized to proceed with ^{125}I-labeling. To allow for the ^{18}F-introduction, the corresponding trimethylammonium- and nitrosubstituted precursors (**10** and **11**) were prepared.

6-Amino-4-[(3-chloro-4-fluorophenyl)amino]quinazoline **5**, the key compound for the synthesis of 6-substituted 4-anilinoquinazolines, was prepared from 4-hydroxyquinazoline **1** according to a described experimental procedure as depicted in Scheme 1 [23].

The amine **5** was subsequently reacted with 3-iodobenzoyl chloride or 4-iodobenzoyl chloride to give *N*-4-[(3-chloro-4-fluorophenyl) amino] quinazoline-6-yl-3-iodobenzamide **6a** and *N*-4-[(3-chloro-4-fluorophenyl) amino] quinazoline-6-yl-4-iodobenzamide **6b**, respectively. These compounds were used in biological studies and also as precursors for the preparation of the stannylated compounds that will be used to prepare the radioiodinated quinazolines (Scheme 2).

Electrophilic substitution is the preferred chemistry route for labeling with radioiodine because of the easy in situ oxidation of iodine to an electropositive form. Electrophilic radiolabeling can be performed by simply adding the oxidant to the appropriate precursor. Although a number of organometallic intermediates can be used, the destannylation reaction is the favorite way to radioiodinate deactivated arenes.

The stannylated compounds **7a** and **7b** were then obtained from their respective iodo-derivatives analogues

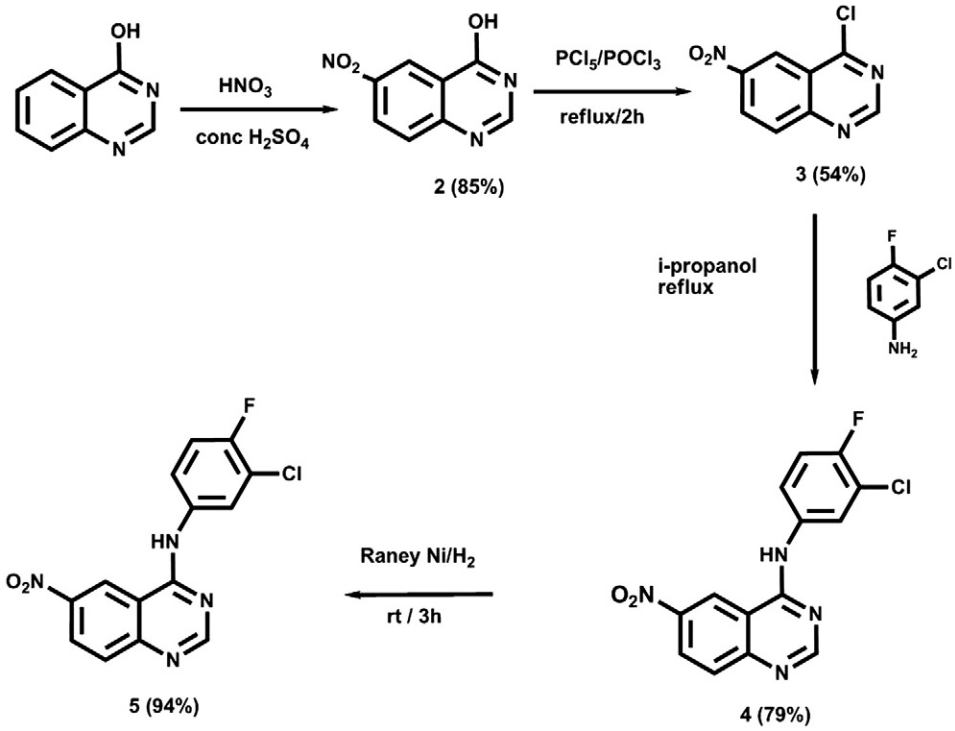

Scheme 1. Chemical synthesis of 6-amino-4-anilinoquinazoline (**5**).

6a and **6b** by a Stille-type cross-coupling reaction. The iodine atom in *N*-{4-[(3-chloro-4-fluorophenyl)amino]quinazoline-6-yl}-3-iodobenzamide (**6a**) and *N*-{4-[(3-chloro-4-fluorophenyl)amino]quinazoline-6-yl}-4-iodobenzamide (**6b**) was substituted by a trimethylstannyl group using hexamethylditin and $Pd(PPh_3)_4$ as a catalyst, as depicted in Scheme 2.

The fluorinated nonradioactive quinazoline *N*-{4-[(3-chloro-4-fluorophenyl)amino]quinazoline-6-yl}-4-fluorobenzamide (**8**) was easily obtained by reaction of the commercially available 4-fluorobenzoyl chloride with 6-amino-4-[(3-chloro-4-fluorophenyl)amino]quinazoline **(5)** and triethylamine as a base, in acetone at room temperature, as depicted in Scheme 3. The fluorinated quinazoline was obtained with high chemical yield (93%) and in high chemical purity and was used for characterization of the radiofluorinated compound and also for biological studies.

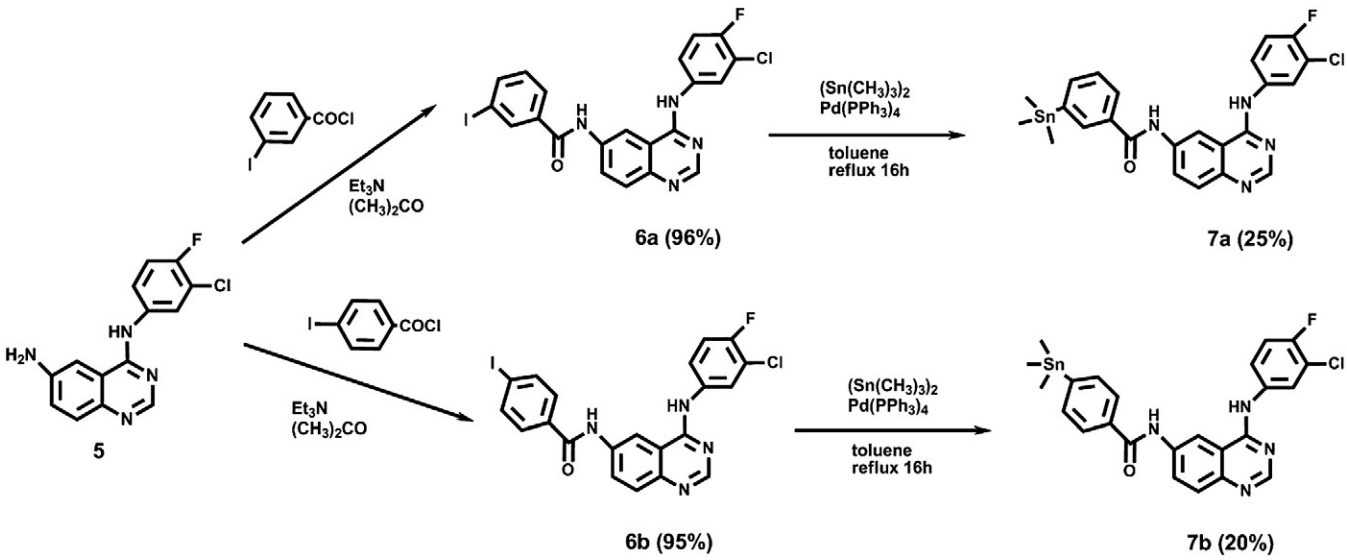

Scheme 2. Chemical synthesis of iodinated 6-substituted 4-anilinoquinazolines (**6a/6b**) and corresponding stannylated analogues (**7a**/**7b**).

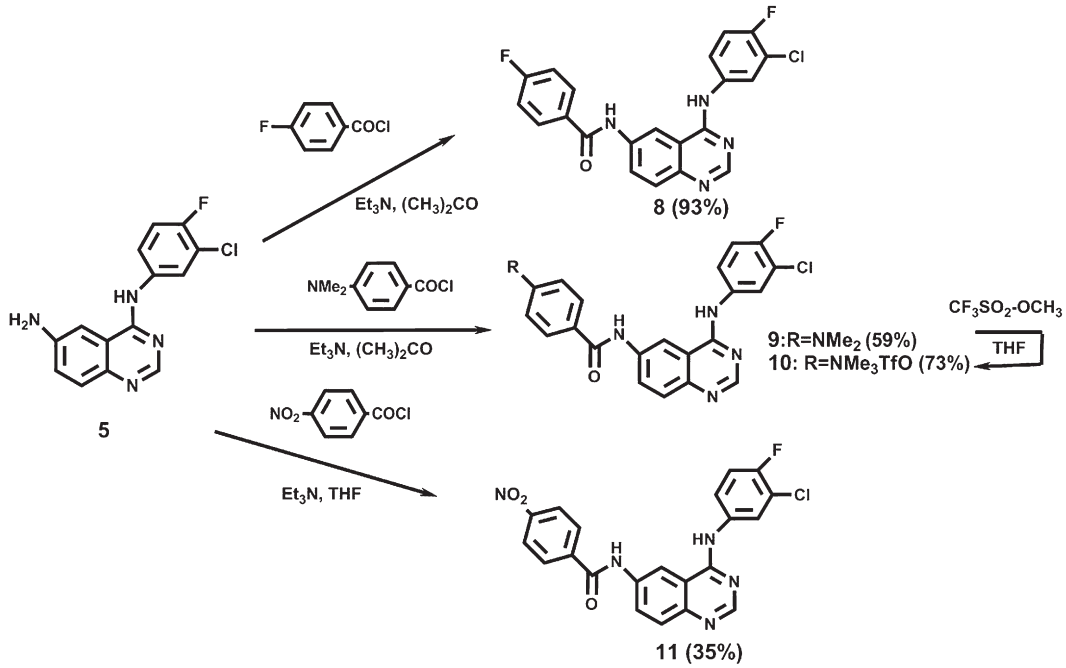

Scheme 3. Chemical synthesis of fluorinated compound (**8**) and precursors for ^{18}F-labeling (**9-11**).

The nucleophilic aromatic n.c.a. ^{18}F-fluorination is the most important route for obtaining ^{18}F-labeled radiopharmaceuticals due to the high metabolic stability of the radiofluorinated aromatic compounds. Nucleophilic aromatic ^{18}F-fluorination calls in the first place for activated aromatic molecules, and therefore, electron withdrawing substituents in *ortho*- or *para*-position to the leaving group appear to be essential. The C4 position of the aromatic ring was chosen for radiofluorination owing to the presence of the carbonyl group at the *para*-position. The introduction of the isotope ^{18}F into the aromatic core may be usually accomplished via nucleophilic substitution of a trimethylammonium or nitro leaving group with [^{18}F] fluoride in aprotic solvents [39].

For the synthesis of the trimethylammonium precursor, 6-amino-4-[(3-chloro-4-fluorophenyl)amino]quinazoline (**5**) was treated with the commercially available 4-(dimethylamino) benzoyl chloride as depicted in Scheme 3 to give the dimethylamino-substituted compound (**9**). Subsequent quaternization with methyl trifluoromethanesulfonate gave the trimethylammonium triflate salt (**10**) in 49% yield.

The corresponding nitro-precursor *N*-{4-[(3-chloro-4-fluorophenyl)amino]quinazoline-6-yl}-4-nitrobenzamide (**11**) was prepared following the same procedure by reacting the commercially available 4-nitro benzoyl chloride with 6-amino-4-[(3-chloro-4-fluorophenyl)amino]quinazoline (**5**) and triethylamine as a base in THF at room temperature (Scheme 3). In this straightforward way, the nitro precursor (**11**) was obtained in 35% chemical yield.

3.2. Radiochemistry

3.2.1. Radioiodination

The radioiodinated compounds *N*-{4-[(3-chloro-4-fluorophenyl)amino]quinazoline-6-yl}-3-[^{125}I]iodobenzamide ([^{125}I]**6a**) and *N*-{4-[(3-chloro-4-fluorophenyl)amino]quinazoline-6-yl}-4-[^{125}I]iodobenzamide ([^{125}I]**6b**) were prepared by electrophilic substitution of the corresponding stannyl precursors **7a** and **7b**. The stannyl derivatives **7a** and

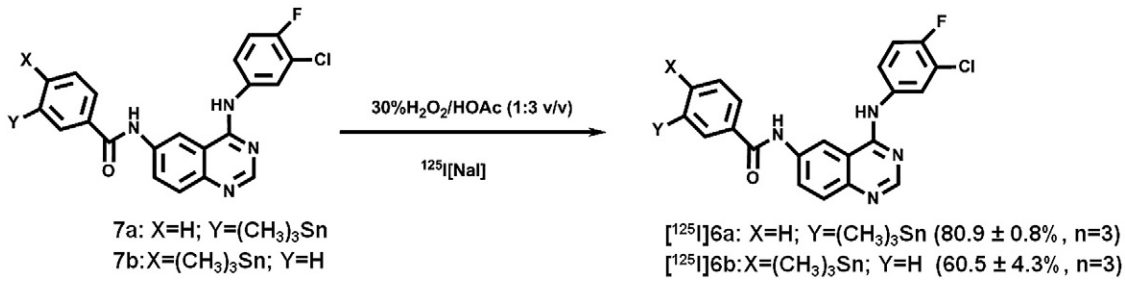

Scheme 4. Synthesis of radioiodinated 6-substituted 4-anilinoquinazolines ([^{125}I]**6a**/[^{125}I]**6b**).

7b were converted to their radioiodinated analogues [^{125}I]**6a** and [^{125}I]**6b** in 80.9%±0.8% (n=3) and 60.5%±4.3% (n=3) radiochemical yield, respectively, by treatment with [^{125I}] NaI in the presence of peracetic acid generated in situ as depicted in Scheme 4 [37].

The crude mixtures were purified by RP-HPLC with simultaneous UV (254 nm) and radioactivity detection by isocratic elution with acetonitrile containing 0.1% TFA and 0.1% aqueous TFA (R_T [^{125}I]**6a**=9.30 min; R_T [^{125}I] **6b**=10.78 min). Using these chromatographic conditions, the radioiodinated compounds are well separated from their nonpolar stannyl counterparts that are eluted at longer retention times (R_T **7a**=13.54 min; R_T **7b**=19.60 min). After RP-HPLC purification, the radiolabeled quinazolines [^{125}I] **6a** and [^{125}I]**6b** were obtained in radiochemical purity higher than 98% after reconstitution in physiological saline (containing 1% Tween-20).

When compared to the corresponding unlabeled analogues, the labeled quinazolines were shown to be the expected products on the basis of their HPLC elution profile. Moreover, the experimental HPLC conditions used in the purification allowed to obtain [^{125}I]**6a/6b** with high radiochemical purity and high specific activity. Since no UV detection at the most sensitive detector setting was observed for the purified labeled compounds, it was then assumed that their specific activity was in the same range as that of the starting [^{125}I]NaI, 2200Ci/mmol.

3.2.2. Radiofluorination

The synthesis of the ^{18}F-radiolabeled quinazoline [^{18}F] **8** was tried via two distinct approaches. In the first one, the corresponding trimethylammonium-precursor **10** has been reacted with [^{18}F]fluoride and K_2CO_3/Kryptofix in aprotic solvents like DMF, DMSO and acetonitrile at temperatures ranging from 90°C to 140°C to insert the radiolabel by nucleophilic aromatic substitution. Unfortunately, the desired compound [^{18}F]**8** was not detected on the radio-HPLC, which means that all the radiolabeling attempts were unsuccessful. This was rather unexpected because the trimethylammonium moiety is known to be a good leaving group and the formation of the precursor containing the trimethylated cation of **10** was confirmed by ESI mass spectroscopy (m/z=450.0, $[M]^+$).

Consequently, the attempts of radiolabeling by nucleophilic substitution with [^{18}F]fluoride were continued with the nitrosubstituted quinazoline precursor **11**. In this case, using DMSO as the solvent and reaction temperatures of about 160°C, the radiolabeled product [^{18}F]**8** was formed in 4.35±0.43% (n=3) radiochemical yield as determined by HPLC, R_T=8.40 min [CH_3CN/0.1% aqueous TFA (55/45)].

From these drastic labeling conditions, it can be concluded that nucleophilic substitution with [^{18}F]fluoride on this specific aromatic system is mainly hampered. Apparently, the electron distribution is different from an ordinary aromatic system, and the electron withdrawing effect of the carbonyl group is resolved by the electron excess of the quinazoline system.

To circumvent this drawback, we have decided to test a different labeling approach using a bifunctional labeling agent, the *N*-succinimidyl 4-[^{18}F]fluorobenzoate [^{18}F]SFB, for introduction of ^{18}F. This activated ester is mainly used for coupling with the amino functions of peptides and proteins to form stable amides under aqueous conditions and can be produced by an automated module-assisted radiosynthesis [36]. Following this approach, we have reacted the amine **5** with [^{18}F]SFB in a mixture of DMSO and various buffers, with and without addition of triethylamine. Unfortunately, even using this strategy, the amide [^{18}F]**8** was not

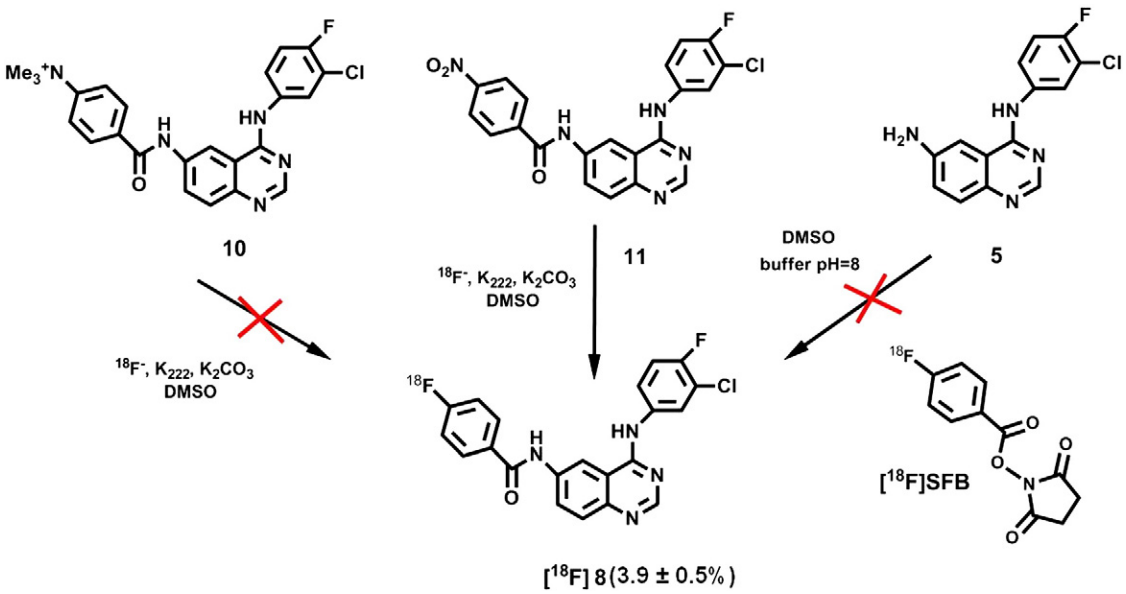

Scheme 5. Synthesis of radiofluorinated 6-substituted 4-anilinoquinazoline ([^{18}F]**8**).

formed. Moreover, using more alkaline conditions by addition of triethylamine or a buffer with pH>9 led to [^{18}F]SFB decomposition (Scheme 5).

3.3. Human serum protein binding, in vitro stability studies and lipophilicity estimation

Protein binding affects the tissue distribution and blood clearance of every compound and its uptake by the target organ. Thus, the extent of this nonspecific binding at various time intervals (0, 1, 2, 4, 24 h) has been estimated in vitro by incubation of radioiodinated quinazolines [^{125}I]**6a** and [^{125}I]**6b** in fresh human serum at 37°C followed by precipitation of the plasmatic proteins with ethanol and comparison of the radioactivity in the precipitate with the radioactivity in the supernatant to give the percentage of radiolabeled compound bound to proteins [40]. Although this method should not be used for an accurate measuring of full protein binding since some disruption of the binding can occur during ethanol precipitation–extraction, it can provide a useful prediction of protein binding and also allows to determine the stability in human serum.

Data from these studies indicated a low percentage of radioiodinated compounds [^{125}I]**6a** and [^{125}I]**6b** bound to the plasmatic proteins (<10%, 24 h), suggesting a low nonspecific binding. By RP-HPLC analysis, only radioiodinated compound was detected in the supernatant, demonstrating the high in vitro stability of [^{125}I]**6a** and [^{125}I]**6b** in human serum towards deiodination up to 24-h incubation at 37°C. The in vitro stability of a radioiodinated compound under physiological conditions is a very important factor to be taken into account in the evaluation of its clinical potential since dehalogenation leads to free iodide, which would result in undesirable biodistribution of radioactivity. High radiochemical stability of [^{125}I]**6a** and [^{125}I]**6b** in physiological saline solution (with 1% Tween-20) was also found up to 24 h at 4°C and 37°C.

The lipophilicity of compounds can affect their tissue permeability properties, which can impair their localization in target tissues. Lipophilicity may also affect binding to low-affinity nonspecific sites that can compromise target tissue to background tissue ratios. The octanol/water partition coefficients of the quinazoline compounds were estimated by a reversed-phase HPLC method [38]. The estimated values indicated that all the compounds are highly lipophilic (log $P_{o/w}$=5.58, 4.83 and 4.55 for **6a**, **6b** and **8**, respectively).

3.4. Biological evaluation

3.4.1. Inhibition of EGFR autophosphorylation

The inhibitory effect of the halogenated quinazolines **6a**, **6b** and **8** upon EGFR autophosphorylation was assessed by Western blot, as described in the experimental section. A431 cells were incubated with concentrations of the quinazolines from 0.1 to 5 μM for 1 h and then stimulated with EGF. Cells stimulated with EGF but without any quinazoline incubation were considered as the positive control and represented 100% of autophosphorylation. By densitometry analysis, the most potent inhibitor was shown to be the fluorinated quinazoline **8** with an IC_{50}<0.1 μM (Fig. 3). Regarding the iodinated quinazolines, **6b** was shown to be a more potent inhibitor of EGFR autophosphorylation than **6a**, with IC_{50} values between 0.1 and 0.5 μM and IC_{50} between 0.5 and 1 μM, respectively.

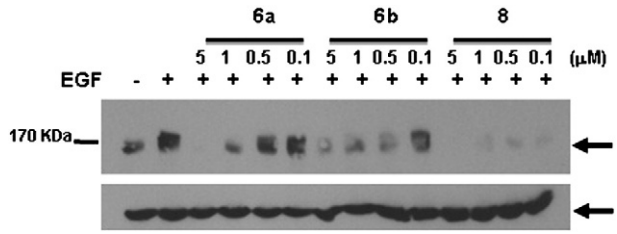

Fig. 3. EGFR autophosphorylation in A431 cells after incubation with quinazolines for 2 h. Total cellular protein extracts were prepared after stimulation with EGF and submitted to a Western blot with an anti-phosphotyrosine antibody. Controls consisted of wells without quinazoline derivatives and with or without EGF. Actin was used as an internal loading control.

3.4.2. Inhibition of tumor cell proliferation

The potency to inhibit A431 cell proliferation of the three halogenated quinazolines was assessed by the MTT colorimetric assay. This assay requires that the compounds are able to penetrate the cell membrane of the intact cells and measures the amount of tetrazolium dye (MTT) reduced to purple formazan salt by mitochondrial dehydrogenase, an enzyme located in the inner mitochondrial membrane of viable cells that is involved in the oxidative phosphorylation. So, cell viability is proportional to the reduction of MTT. The proliferation inhibitory activity of the quinazoline derivatives was evaluated by the IC_{50}, which is the concentration needed to inhibit cell proliferation by 50%, determined through dose–response curves achieved from percentage of cell proliferation plotted against the corresponding compound concentration (Fig. 4). IC_{50} values are presented in Table 1.

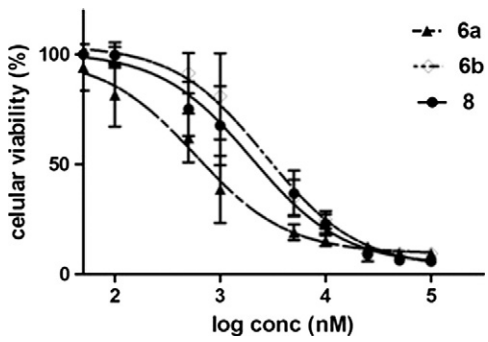

Fig. 4. Inhibition of A431 cells proliferation by quinazolines **6a**, **6b** and **8** (n=3).

Table 1
Inhibition of A431 cell proliferation by quinazoline derivatives (n=3)

Compound	Inhibition of cell proliferation IC_{50} (μM) (n=3)
6a	0.78±0.02
6b	3.37±0.17
8	2.43±0.13

Analysis of these data indicated that all the halogenated compounds are able to cross the cell membrane, as expected from their lipophilic character, and inhibit A431 cell proliferation. The IC_{50} values below 3.5 μM demonstrate that they are potent inhibitors. The most potent one was found to be the iodinated quinazoline **6a**.

By contrast, the fluorinated derivative **8** and the iodinated quinazoline **6b** were proven to be less potent inhibitors of cell proliferation than **6a** in spite of their higher ability to inhibit EGFR autophosphorylation. This discrepancy may result from the lower aqueous solubility of **6b** and **8** compared to **6a**.

3.4.3. Cellular uptake studies

Cellular uptake studies of the radioiodinated quinazolines were undertaken to evaluate their level of internalization in A431 cells after the radiolabeling procedure, an important parameter to assess their usefulness as probes for EGFR-TK molecular imaging. The uptake kinetics of [^{125}I]**6a** and [^{125}I]**6b** at 37°C is presented in Fig. 5.

Data indicate that both iodinated quinazolines present a similar cell uptake pattern with an overall percentage relatively high (>35%). They are rapidly taken by the cells (19.6%±0.6% and 18.8%±3.2%/10^6 cells at 15 min for [^{125}I]**6a** and [^{125}I]**6b**, respectively), with a pronounced increase of total cell uptake over time. This behavior reflects the high lipophilic character of the compounds and is in agreement with the found ability of the iodinated compounds to inhibit cell proliferation.

Altogether, these results with EGFR overexpressing cells suggest that the compounds [^{125}I]**6a** and [^{125}I]**6b** are promising candidates as EGFR SPECT imaging probes.

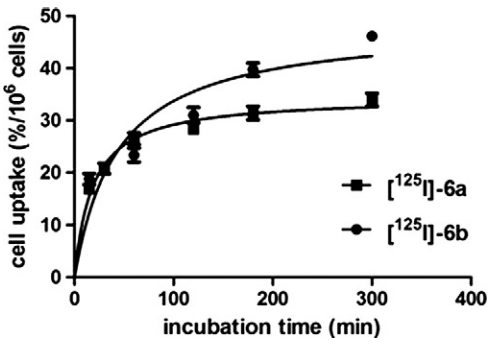

Fig. 5. Cellular uptake kinetics of [^{125}I]**6a** and [^{125}I]**6b** in A431 cells at 37°C in humidified 5% CO_2 atmosphere (n=4).

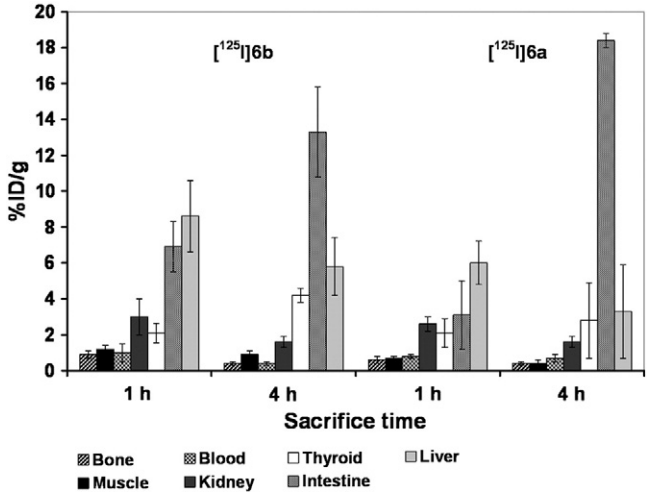

Fig. 6. Biodistribution data in the most relevant organs, expressed as % ID/g organ, for radioiodinated quinazolines [^{125}I]**6a** and [^{125}I]**6b** at 1 and 4 h after administration in female CD-1 mice (n=4).

3.4.4. Biodistribution studies

Biodistribution studies of [^{125}I]**6a** and [^{125}I]**6b** were carried out in healthy CD-1 mice at 1 and 4 h to get a first insight on the in vivo stability and on the biokinetics profile of the radioiodinated compounds. Results of these studies are summarized for the most relevant organs in Fig. 6.

The biodistribution profiles of both compounds are quite similar, following the tendency in agreement with the usual pattern of most radiolabeled anilinoquinazolines that have been described so far [24–28]. The main features of the in vivo behavior of [^{125}I]**6a** and [^{125}I]**6b** are the relatively fast clearance from blood (0.8%±0.1% injected dose (ID)/g and 1.0%±0.5% ID/g, respectively, at 1 h p.i.) and muscle (0.7%±0.1% ID/g and 1.2%±0.2% ID/g, respectively, at 1 h p.i.) and high liver uptake that clears into the intestines where the activity increases over time.

These findings suggest that excretion occurs mainly via the hepatobiliary tract, a pattern of excretion most likely due to the high lipophilicity of the compounds. Nevertheless, there is a small contribution of the urinary tract (2.6%±0.4% ID/g and 3.0%±1.0% ID/g kidney, at 1 h p.i., respectively, for [^{125}I]**6a** and [^{125}I]**6b**, which decrease to 1.6%±0.3% ID/g and 1.6%±0.3% ID/g kidney at 4 h). The main differences are related to a slightly faster hepatobiliary excretion of [^{125}I]**6a** than [^{125}I]**6b**. At 4 h p.i., there is no noteworthy radioactivity retention in any other organ, except those involved in the excretory route (predominantly intestines).

The in vivo stability of the radioiodinated compounds was evaluated by measuring the thyroid radioactivity concentration, since free radioiodide resulting from in vivo deiodination is almost immediately taken by this organ. The low thyroid radioactivity levels (0.06%±0.01% ID and 0.15%±0.05% ID/ thyroid, at 1 h p.i., respectively, for [^{125}I]**6a** and [^{125}I]**6b**, which increase to 0.20%±0.08%

ID and 0.31%±0.04% ID/thyroid at 4 h) compared to our previously reported radioiodinated quinazolines led us to conclude that both radioiodinated compounds are stable in vivo [23].

Regardless of the promising cellular data and the high in vivo stability, the high level of radioactivity in the hepatobiliary tract discouraged us to proceed to studies in tumor-bearing mice since it would lead to the misinterpretation of the images. Nevertheless, this study suggests that these quinazoline derivatives are promising EGFR-TKI-based probes and are worth further exploration in order to promote a more rapid elimination from the hepatobiliary tract.

4. Conclusion

We have successfully prepared three novel halogenated 4-anilinoquinazoline-based EGFR-TKIs: **6a**, **6b** and **8**. The in vitro inhibition study of EGFR autophosphorylation and A431 cell proliferation proved that all three compounds show inhibitory properties at the micromolar level, clearly maintaining the inhibition ability of the parent compound **5** [23,24]. The radioiodinated analogues [^{125}I]**6a** and [^{125}I]**6b** were synthesized in high radiochemical yield and radiochemical purity. With this radiolabeling approach, it was possible to introduce the radiohalogen at the last step of the synthetic procedure without changing the lead structure. These radioiodinated compounds were highly taken up by A431 cells, and their biodistribution profile in healthy mice indicated a rapid blood and muscle clearance, with excretion occurring mainly via the hepatobiliary tract as expected from their highly lipophilic character.

The synthesis of the ^{18}F-radiolabeld anilinoquinazoline [^{18}F]**8** was attempted by nucleophilic substitution of the trimethylammonium- and nitrosubstituted anilinoquinazoline precursors **10** and **11**, respectively, and additionally by coupling of the amino compound **5** with the bifunctional labeling agent [^{18}F]SFB. Despite all the effort, [^{18}F]**8** was formed in only a poor labeling yield of 4% maximum as detected in analytical HPLC when the nitro precursor **11** was used. For that reason, no further radiopharmacological investigation of [^{18}F]**8** was undertaken. This was much more regrettable because the fluorinated nonradioactive compound **8** seemed to be the most potent inhibitor of EGFR autophosphorylation. In future work, other functional groups at C6 should be explored in order that the nucleophilic aromatic substitution with [^{18}F]fluoride could be facilitated. It has to be proven that these modifications will not have a negative impact on the properties of the anilinoquinazoline as EGFR TKI.

In conclusion, data from this study suggest that these quinazolines derivatives can act as EGFR-TKI, warranting further modifications in chemical structure in order to be explored as potential probes for SPECT and PET.

Acknowledgments

The authors gratefully acknowledge Deutscher Akademischer Austausch Dienst/Fundação para a Ciência e Tecnologia (DAAD/FCT) (0811983/441.00) for financial support and Dr. Joaquim Marçalo for mass spectra analysis. C. Neto thanks FCT for a Ph.D. grant (SFRH/BD/31319/2006). The ESI/QITMS instrument was acquired with the support of the Programa Nacional de Reequipamento Científico (Contract REDE/1503/REM/2005-ITN) of FCT and is part of Rede Nacional de Espectrometria Massa (RNEM).

References

[1] Laskin JJ, Sandler AB. Epidermal growth factor receptor: a promising target in solid tumours. Cancer Treat Rev 2004;30:1–17.
[2] Bublil EM, Yarden Y. The EGF receptor family: spearheading a merger of signalling and therapeutics. Curr Opin Cell Biol 2007;19:124–34.
[3] Herst RS. Review of epidermal growth factor receptor biology. Int J Radiat Oncol Biol Phys 2004;59:21–6.
[4] Levitzki A. Protein kinase inhibitors as a therapeutic modality. Acc Chem Res 2003;36:462–9.
[5] Noble MEM, Endicott JA, Johnson LN. Protein kinase inhibitors: insights into drug design from structure. Science 2004;303:1800–5.
[6] Tibes R, Trent J, Kurzrock R. Tyrosine kinase inhibitors and the dawn of molecular cancer therapeutics. Ann Rev Pharm Toxicol 2005;45:357–84.
[7] Workman P. Genomics and the second golden era of cancer drug development. Mol Biosyst 2005;1:17–26.
[8] Breza N, Pato' J, Orfi L, Hegymegi-Barakonyi B, Anhegyi PB, Varkondi E, et al. Synthesis and characterization of novel quinazoline type inhibitors for mutant and wild-type EGFR and RICK kinases. J Recept Signal Transduct 2008;28:361–73.
[9] Allen LF, Eiseman IA, Fry DW, Lenehan PF. CI-1033, an irreversible pan-erbB receptor inhibitor and its potential application for the treatment of breast cancer. Semin Oncol 2003;30:65–78.
[10] Arora A, Scholar EM. Role of tyrosine kinase inhibitors in cancer therapy. J Pharmacol Exp Ther 2005;315:971–99.
[11] Montemurro F, Valabrega G, Aglietta M. Lapatinib: a dual inhibitor of EGFR and HER2 tyrosine kinase activity. Expert Opin Biol Ther 2007;7(2):257–68.
[12] Medina PJ, Goodin S. Lapatinib: a dual inhibitor of human epidermal growth factor receptor tyrosine kinases. Clin Ther 2008;30(8):1426–47.
[13] Albanell J, Gascón P. Small molecules with EGFR-TK inhibitor activity. Curr Drug Targets 2005;6:259–74.
[14] Bikker JA, Brooijmans N, Wissner A, Mansour TS. Kinase domain mutations in cancer. Implications for small molecule drug design strategies. J Med Chem 2009;52:1493–509.
[15] Pal A, Glekas A, Doubrovin M, Balatoni J, Beresten T, Maxwell D, et al. Molecular imaging of EGFR kinase activity in tumours with ^{124}I-labeled small molecular tracer and Positron emission tomography. Mol Imaging Biol 2006;8:262–77.
[16] Mishani E, Abourbeh G. Cancer molecular imaging: radionuclide-based biomarkers of the epidermal growth factor receptor (EGFR). Curr Top Med Chem 2007;7:1755–72.
[17] Mishani E, Abourbeh G, Eiblmaier M, Anderson CJ. Imaging of EGFR and EGFR tyrosine kinase overexpression in tumors by nuclear medicine modalities. Curr Pharm Des 2008;14:2983–98.
[18] Gelovani JG. Molecular imaging of epidermal growth factor receptor expression–activity at the kinase level in tumors with positron emission tomography. Cancer Metastasis Rev 2008;27:645–53.

[19] Pantaleo MA, Nannini M, Maleddu A, Fanti S, Ambrosini V, Nanni C, et al. Conventional and novel PET tracers for imaging in oncology in the era of molecular therapy. Cancer Treat Rev 2008;34:103–21.
[20] Pantaleo MA, Nannini M, Maleddu A, Fanti S, Nanni C, Boschi S, et al. Experimental results and related clinical implications of PET detection of epidermal growth factor receptor (EGFr) in cancer. Ann Oncol 2009;20:213–26.
[21] Hicks JW, VanBrocklin HF, Wilson AA, Sylvain H, Vasdev N. Radiolabeled small molecule protein kinase inhibitors for imaging with PET or SPECT. Molecules 2010;15:8260–78.
[22] Pantaleo MA, Mishani E, Nanni C, Landuzzi L, Boschi S, Nicoletti G, et al. Evaluation of modified PEG-anilinoquinazoline derivatives as potential agents for EGFR imaging in cancer by small animal PET. Mol Imaging Biol 2010;12:616–25 SPECT.
[23] Fernandes C, Oliveira C, Gano L, Bourkoula A, Pirmettis I, Santos I. Radioiodination of new EGFR inhibitors as potential SPECT agents for molecular imaging of breast cancer. Bioorg Med Chem 2007;15: 3974–80.
[24] Fernandes C, Santos IC, Santos I, Pietzsch HJ, Kunstler JU, Kraus W, et al. Rhenium and technetium complexes bearing quinazoline derivatives: progress towards a ^{99m}Tc biomarker for EGFR-TK imaging. Dalton Trans 2008;28:3215–25.
[25] Bourkoula A, Paravatou-Petsotas M, Papadopoulos A, Santos I, Pietzsch HJ, Livaniou E, et al. Synthesis and characterization of rhenium and technetium-99m tricarbonyl complexes bearing the 4-[3-bromophenyl]quinazoline moiety as a biomarker for EGFR-TK imaging. Eur J Med Chem 2009;44:4021–7.
[26] Garcia R, Fousková P, Gano L, Paulo A, Campello P, Toth E, et al. A quinazoline-derivative DOTA-type gallium(III) complex for targeting epidermal growth factor receptors: synthesis, characterisation and biological studies. J Biol Inorg Chem 2009;14:261–71.
[27] Garcia R, Kubıcek V, Drahos B, Gano L, Santos IC, Campello P, et al. Synthesis, characterization and biological evaluation of In(III) complexes anchored by DOTA-like chelators bearing a quinazoline moiety. Metallomics 2010;2:571–80.
[28] Hirata M, Kanai Y, Naka S, Matsumuro K, Kagawa S, Mitsuyoshi Y, et al. Evaluation of radioiodinated quinazoline derivative as a new ligand for EGF receptor tyrosine kinase activity using SPECT. Ann Nucl Med 2011;25:117–24.
[29] Bonasera TA, Ortu G, Rozen Y, Krais R, Freedman NM, Chisin R, et al. Potential (18)F-labeled biomarkers for epidermal growth factor receptor tyrosine kinase. Nucl Med Biol 2001;28:359–74.
[30] Ortu G, Ben-David B, Rozen Y, Freedman NMT, Chisin R, Levitski A, et al. Labeled EGFr-TK irreversible inhibitor (ML03): in vitro and in vivo properties, potential as PET biomarker for cancer and feasibility as anticancer drug. Int J Cancer 2002;101:360–70.
[31] Ben-David I, Rozen Y, Ortu G, Mishani E. Radiosynthesis of ML03, a novel positron emission tomography biomarker for targeting epidermal growth factor receptor via the labeling synthon: [^{11}C]acryloyl chloride. Appl Radiat Isot 2003;58:209–17.
[32] Shaul M, Abourbeh G, Jacobson O, Rozen Y, Laky D, Levitzki A, et al. Novel iodine-124 labeled EGFR inhibitors as potential PET agents for molecular imaging in cancer. Bioorg Med Chem 2004;12:3421–9.
[33] Mishani E, Abourbeh G, Rozen Y, Jacobson O, Laky D, Ben DI, et al. Novel carbon-11 labeled 4-dimethylamino-but-2-enoic acid [4-(phenylamino)-quinazoline-6-yl]-amides: potential PET bioprobes for molecular imaging of EGFR-positive tumors. Nucl Med Biol 2004; 31:469–76.
[34] Mishani E, Abourbeh G, Rozen Y, Jacobson O, Dissoki S, Daniel RB, et al. High-affinity epidermal growth factor receptor (EGFR) irreversible inhibitors with diminished chemical reactivities as positron emission tomography (PET)-imaging agent candidates of EGFR overexpressing tumors. J Med Chem 2005;48:5337–48.
[35] Dissoki S, Laky D, Mishani E. Fluorine-18 labeling of ML04 — presently the most promising irreversible inhibitor candidate for visualization of EGFR in cancer. J Labelled Comp Radiopharm 2006; 49:533–43.
[36] Maeding P, Fuechtner F, Wuest F. Module assisted synthesis of the bifunctional labelling agent *N*-succinimidyl 4-[^{18}F]fluorobenzoate ([^{18}F]SFB). Appl Radiat Isot 2005;63:329–32.
[37] Veach DR, Namavaria M, Beresten T, Balatoni J, Minchenko M, Djaballah H, et al. Synthesis and in vitro examination of [^{124}I]-, [^{125}I]- and [^{131}I]-2-(4-iodophenylamino) pyrido[2,3-d]pyrimidin-7-one radiolabeled Abl kinase inhibitors. Nucl Med Biol 2005;32:313–21.
[38] Minick D, Frenz J, Patrick M, Brent D. A comprehensive method for determining hydrophobicity constants by reversed phase high-performance liquid chromatography. J Med Chem 1988;31:1923–33.
[39] H.H. Coenen, Fluorine-18 labelling methods: features and possibilities of basic reactions. In: P.A. Schubiger, L. Lehmann, M. Friebe, editors. PET chemistry — the driving force in molecular medicine. Ernst Schering Research Foundation Workshop 62, Springer: Berlin, Heidelberg, New York: 2007, p. 15–50.
[40] Eisenwiener K-P, Prata MIM, Buschmann I, Zhang H-W, Santos AC, Wenger S, et al. Bioconjugate Chem 2002;13:530–41.